A continuous biofilm process for enhanced biological nitrogen and phosphorus removal with alternating flow direction and carbon

Journal of Water Process Engineering 88 (2026) 110186

Contents lists available at ScienceDirect

Journal of Water Process Engineering

journal homepage: www.elsevier.com/locate/jwpe

A continuous biofilm process for enhanced biological nitrogen and phosphorus removal with alternating flow direction and carbon management

E. Ossiansson [a,c], M. Piculell [b], D.J.I. Gustavsson [a], S. Bengtsson [a], M. Christensson [b], C. Rosen [b], F. Persson [c,*]

[a] VA SYD, Box 191, SE-20121, Malmö, Sweden
[b] Veolia - AnoxKaldnes Technologies, Klosterängsvägen 11A, SE-22647, Lund, Sweden
[c] Chalmers University of Technology, Dept. of Architecture and Civil Engineering, SE-41296, Gothenburg, Sweden

ARTICLE INFO

Editor: Di Wu

Keywords:
Enhanced biological phosphorus removal (EBPR)
Moving bed biofilm reactor (MBBR)
Volatile fatty acids (VFA)
Polyphosphate accumulating organisms (PAO)

ABSTRACT

More compact wastewater treatment is attractive for handling increased loads and stricter effluent requirements. The moving bed biofilm reactor (MBBR) can achieve high carbon and nitrogen removal capacity at a small footprint but is challenged to also reach efficient enhanced biological phosphorus removal (EBPR). This pilot study evaluated a new approach to promote EBPR and high nitrogen removal in continuous flow MBBRs by operating with alternating flow direction and intermittent aeration, thus enabling the cyclic anaerobic and aerobic/anoxic conditions required for polyphosphate accumulating organisms (PAOs). The MBBRs utilised a novel bio-based support material with external biofilm growth for improved mass transfer and were fed pre-filtered municipal wastewater. To increase the availability of readily biodegradable carbon for nutrient removal, the influent was supplied with volatile fatty acids (VFA), mimicking fermentation of sludge from primary filtration. The 460-day long study demonstrated stable nitrogen removal and EBPR. The presence of PAOs in the biofilm was demonstrated in batch tests as well as by microbial analysis, with *Ca.* Phosphoribacter, *Tetrasphaera* and *Ca.* Accumulibacter being detected in high relative abundances. Both aerobic and anoxic phosphate uptake were observed, indicating denitrifying PAO activity. The VFA addition had a strong impact on the EBPR, which increased when directing the VFA to the anaerobic phases, compared to dosing VFA continuously. With VFA dosing in the anaerobic phases, nitrogen and phosphorus removal were 84 ± 5% and 68 ± 18%, respectively, demonstrating the possibilities with this novel process for future full-scale installations.

1. Introduction

Enhanced biological phosphorus removal (EBPR) is an alternative to chemical precipitation for phosphorous removal in wastewater treatment. EBPR relies on utilizing the ability of polyphosphate accumulating organisms (PAOs) to grow and take up excess phosphorus, which they store within their cells as polyphosphate. EBPR, in combination with nitrogen removal, is widely applied in different kinds of activated sludge processes [1], but since many wastewater treatment plants (WWTPs) face increased loads and stricter effluent requirements at limited footprints, more compact treatment processes with EBPR and nitrogen removal are required [2].

The moving bed biofilm reactor (MBBR) is a well-established, compact biofilm process for wastewater treatment. With MBBR, there is no need for granulation, while the continuous detachment of biomass from the biofilm surface and lack of sludge retention allows for a high biomass yield and energy recovery potential [3]. EBPR in MBBRs has been shown successful at lab- and pilot scale trials [4–7], but studies combining EBPR with nitrogen removal in MBBRs are scarce, especially those applied at realistic conditions in municipal applications with varying temperature and flow rate.

A main challenge when applying EBPR and nitrogen removal in

* Corresponding author.
E-mail addresses: elin.ossiansson@nsva.se (E. Ossiansson), maria.piculell@veolia.com (M. Piculell), david.gustavsson@vasyd.se (D.J.I. Gustavsson), simon.bengtsson@vasyd.se (S. Bengtsson), magnus.christensson@veolia.com (M. Christensson), christian.rosen@veolia.com (C. Rosen), frank.persson@chalmers.se (F. Persson).

https://doi.org/10.1016/j.jwpe.2026.110186
Received 27 February 2026; Received in revised form 17 April 2026; Accepted 4 May 2026
Available online 11 May 2026

MBBR processes, where the biomass typically resides in a specific reactor, lies in obtaining alternating anaerobic and anoxic/aerobic conditions for the same biomass. Creative solutions to this challenge include moving biofilm carriers between aerated and anaerobic zones [8], lifting the biofilm up in the air intermittently [9], or operation as sequencing batch biofilm reactors (SBBRs) with aerated and non-aerated phases [10–12]. Lifting or moving biofilm carriers is indeed feasible but requires dedicated equipment, and the need for additional equalising volumes in SBBRs is a drawback compared to continuous processes.

One way to obtain alternating redox conditions in a continuous biofilm process would be to operate two coupled reactors with intermittent aeration and alternating flow direction. This would also enable flexibility to optimise the process and prioritise between nitrogen and phosphorus removal. Operation with alternating flow direction is well-established for activated sludge processes [13], and the inclusion of EBPR in the alternating flow process by adding an anaerobic phase after the denitrification has been implemented at full-scale [14,15]. For biofilm systems, attempts have been made to use fixed biofilm for EBPR in alternating reactors [16–18], but for these systems the fixed biofilm had to be washed in a separate step to extract the phosphorus-rich biomass. This extra step could be avoided by instead applying MBBR, where biomass continuously detach from the biofilm carriers, which would facilitate biological phosphorous removal, but so far, the combination of MBBR with alternating flow direction for EBPR has not been studied.

Another vital factor for successful EBPR, especially when combining it with nitrogen removal, is the availability of sufficient amounts of readily biodegradable carbon. For biofilm processes, where particles are washed out relatively fast compared to the activated sludge process, hydrolysis and fermentation of the influent carbon has been identified as the rate limiting step for EBPR [19,20]. Thus, for an influent wastewater low in readily biodegradable carbon, the addition of external carbon source might be necessary for a biofilm process to achieve stable and high EBPR [4,21]. Another means to provide the required amount of accessible carbon would be to produce volatile fatty acids (VFAs) by primary sludge fermentation. Chemically enhanced primary filtration, which has the potential of high removal of total suspended solids (TSS) [22], can be combined with sludge fermentation for production of VFAs, which in turn can be dosed back to the main process line [23–25]. Fermentation of primary sludge at ambient temperature (16–29 °C) and five days retention time can produce enough carbon source to nearly double the VFA concentration of influent wastewater [25]. With such side-stream fermentation, produced VFAs can be stored and dosed in a controlled manner to the process on demand. As VFAs can be taken up during both the anoxic and the anaerobic phases in the reactors, carbon management by dosage of VFA solely to the anaerobic phase may favour PAOs and phosphorus removal. Although this type of primary treatment for carbon management may be effective for a carbon-limited biofilm process, especially when operating with alternating flow direction, it has not yet been investigated.

This study evaluates a novel continuous biofilm process for nitrogen removal and EBPR operating with intermittent aeration and alternating flow direction. The influent wastewater to the MBBR process is pre-treated (*i.e.* primary filtration and VFA dosage) to enable carbon management. With this combination, previous challenges to achieve EBPR in MBBRs are mitigated, as there is no need to move the support material between the reactors, no requirement of internal recirculation pumps or buffer tanks, and VFA can be directed for anaerobic uptake by the PAOs. In addition, the MBBRs use a new bio-based support material with a large external surface area for biofilm growth to enable high volumetric removal and continuous detachment of biofilm biomass. The aim of the study was to obtain EBPR while also achieving efficient nitrogen removal (>80%) for municipal wastewater treatment at field conditions, and to evaluate the impact of phase control, loading rates and control strategies for VFA addition on nutrient removal by studies in pilot scale. To assess composition and activity of the nitrogen and phosphorous converting microorganisms, amplicon sequencing and batch activity tests were employed.

2. Materials and methods

The pilot plant was located at Källby municipal WWTP in Lund, Sweden, and consisted of a chemically enhanced primary filtration step [24,25] followed by a continuous biofilm process in two MBBR reactors operating in cycles with alternating flow direction, intermittent aeration and VFA dosing corresponding to VFA production from primary sludge fermentation (Fig. 1). The study lasted for 460 days, divided into six distinct periods with different operating conditions (Table 1).

2.1. Primary filtration

Influent wastewater, after screening at the main WWTP, was pumped to the primary filtration pilot unit at a flow rate of 7–18 m^3/h, proportional to the main WWTP flow rate. Polymer (Superfloc 6260, Kemira Kemi AB) was added as a 0.1–0.2% solution to the flocculation prior to filtration. Two 0.8 m^3 flocculation reactors were operated in series, with mixing at 70 and 50 rpm, respectively. A rotating belt filter (RBF) SF1000 (Salsnes Filter) was operated at a level of 200–210 mm with a 350 μm mesh filter, which was washed with high pressure water three times per day. The filtered wastewater was pumped to a 1000 μm mesh drum filter HDF801 (Hydrotech) (working as a safeguard and reservoir for the subsequent biofilm reactors) at a constant flowrate of ~4 m^3/h. The primary filtration unit was in operation without changes from day 22 onwards.

2.2. Biofilm reactors

Two 0.6 m^3 (depth 0.8 m) MBBRs (R1 and R2) were operated in series with alternating flow direction and intermittent aeration (Fig. 1). The wastewater was pumped from the drum filter to either of the reactors at a flow rate of 1–2 L/min (proportional to the primary treatment inflow), and the average load was varied during the study (see Section 2.5). The reactors were equipped with biofilm support material made from recycled, renewable biomass (Veolia Water Technologies) to enable biofilm growth. The support material differed from conventional MBBR carriers in several aspects. Conventional MBBR carriers are typically in the centimetre size-range, made from high-density polyethylene and moulded or extruded to a pre-defined shape with voids enabling a protected surface area for biofilm growth [26]. The support material used in this study consisted of particles (diameter average 1.4 mm), sourced from dehydrated and mechanically stabilised municipal wastewater sludge. Thus, there was no quantifiable protected surface area on this material, but rather the small size and relatively rugged surface enabled an external biofilm growth. Once colonised with biofilm, the size and shape of the support material changed with the biofilm thickness, which in turn was a result of the load and reactor operating conditions. As the size of the carrier, as well as the biofilm surface area, was varying with biofilm thickness, the conventional way of assessing MBBRs by surface area was not applicable.

Approximately 24 L of dry support material was added to each reactor during start-up. Small amounts of support material were added day 113 and 225 to replace support material that had been lost due to technical problems (Table S1). Once added, the support material swelled in size and was colonised with biofilm.

During operation, the biofilm support material was kept in suspension in the reactors by mechanical mixing and/or aeration. During aeration, the air flow was controlled to keep the dissolved oxygen (DO) concentration > 3 mg/L. The reactors were equipped with online sensors for DO and oxidation reduction potential (LDO2 and pHD respectively, Hach). In addition, ammonium and phosphate were analysed in filtered water from R2 with Amtax and Phosphax (Hach). The sum of nitrite and nitrate (NO_X^--N) was measured online in parallel with the analysers using an NT3100 sensor (Hach).

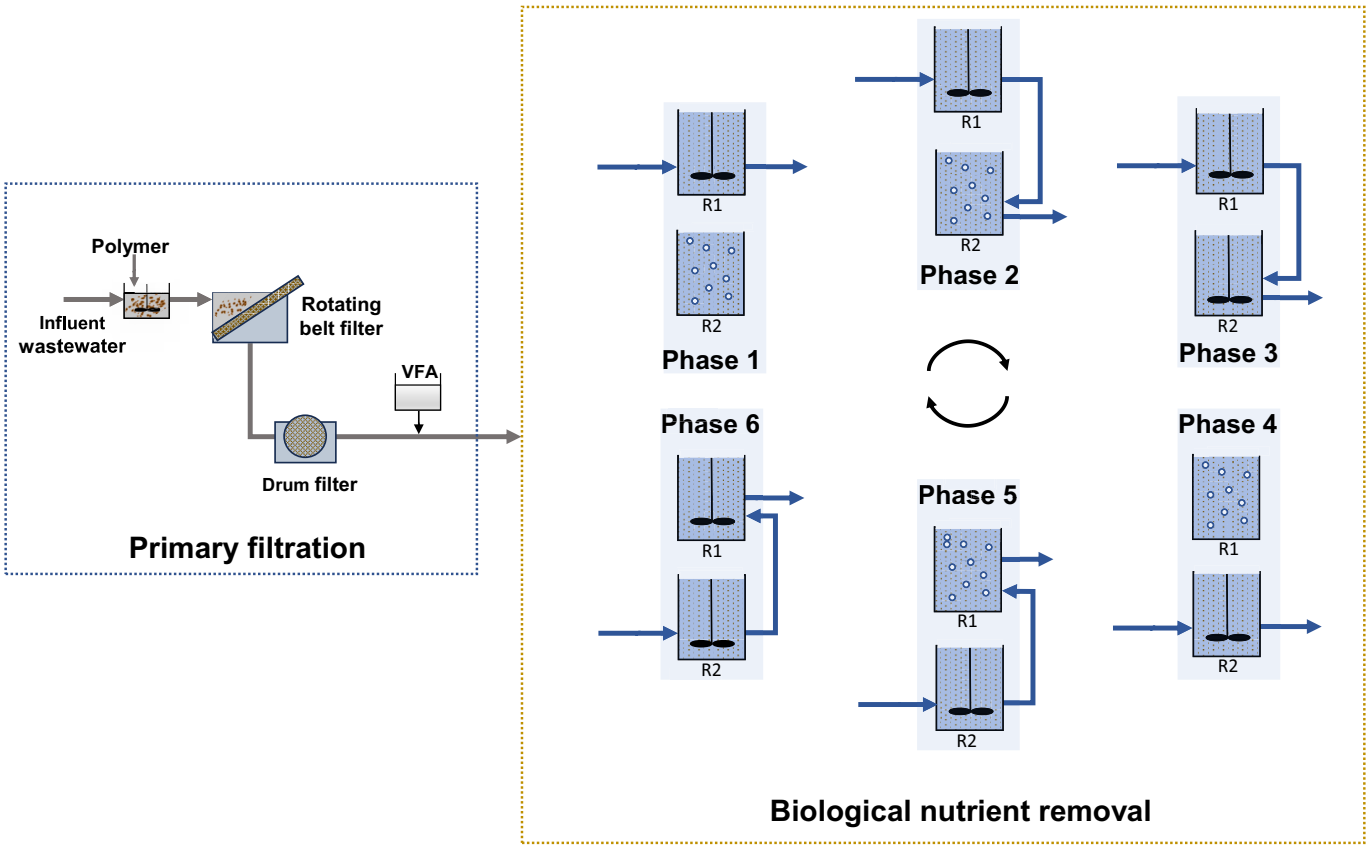

Fig. 1. Overview of the pilot plant, showing pretreatment with primary filtration (left) and operation of the continuous moving bed biofilm reactor (right). The six operating phases are indicated, with alternating water flow and aeration patterns for the two reactors (R1 and R2). The aerated reactor is indicated by white bubbles, the non-aerated reactor with a stirrer.

Table 1
Operational periods for the biofilm reactors, with influent characteristics based on 24 h composite samples, VFA dosage, temperature and HRT (mean ± standard deviation). Influent refers to the wastewater excluding VFA dosing.

Period	A	B	C	D	E	F
Day	1–111	112–135	136–211	211–279	280–380	381–460
Cycle control	Set	Automatic	Set	Automatic	Set	Set
Unaerated time (%)	71	Varying	57–72	Varying	56	71
VFA dosage	Constant	Constant	Constant	Redox, constant	Redox	Redox, constant
Temperature (°C)	17.7 ± 2.0	13.8 ± 1.4	14.4 ± 1.1	16.6 ± 2.6	21.6 ± 1.6	19.0 ± 1.9
HRT (h)	5–14	13.3 ± 1.3	11.5 ± 2.4	12.8 ± 2.6	14.2 ± 1.7	15.7 ± 2.2
Number of samples	38	8	26	24	38	31
Influent N_{tot} (mg/L)	47.6 ± 14.9	32.4 ± 5.3	38.6 ± 8.0	43.8 ± 7.2	47.1 ± 6.5	50.5 ± 9.1
Influent NH_4^+ (mg N/L)	31.9 ± 10.0	20.2 ± 4.1	25.6 ± 6.5	32.8 ± 4.1	34.3 ± 7.0	35.7 ± 7.0
Influent P_{tot} (mg/L)	7.6 ± 4.6	4.4 ± 1.1	4.5 ± 1.1	5.3 ± 0.8	5.9 ± 0.9	5.9 ± 1.2
Influent PO_4^{3-} (mg P/L)	2.9 ± 1.0	1.6 ± 0.4	2.4 ± 0.6	3.2 ± 0.6	3.5 ± 0.6	3.3 ± 0.7
Influent TSS (mg/L)	201 ± 156	136 ± 37	103 ± 58	116 ± 20	120 ± 24	122 ± 34
Influent COD (mg/L)	350 ± 206	232 ± 42	222 ± 73	279 ± 39	293 ± 43	306 ± 57
Influent soluble COD (mg/L)	91 ± 46	56 ± 11	72 ± 20	99 ± 16	103 ± 26	117 ± 23
VFA dosed (mg COD/L influent)	0–50	22 ± 2	27 ± 8	52 ± 55	75 ± 45	44 ± 22

Effluent sieves, typically used in MBBRs to retain carriers, were not applicable for this system due to the small size of the support material. Instead, the reactors were equipped with three-phase separators. By having a density of 1.2 g/cm^3, the support material was retained by gravity, while the suspended solids and detached biofilm were continuously discharged with the effluent wastewater. The effluent was collected in a separate tank for sampling and monitoring of particles (see Section 2.6).

2.3. Phase control

The alternating flow direction strategy for the MBBRs, consisted of a cycle of six operational phases, as described in Fig. 1. R1 received influent wastewater during phases 1–3, while R2 received influent wastewater during phases 4–6. While both reactors were continuously mixed, R1 and R2 were aerated in phases 4–5 and 1–2, respectively. This strategy ensured addition of influent COD during unaerated conditions and allowed for anoxic conditions (denitrification and phosphate uptake by denitrifying PAOs), anaerobic conditions (carbon uptake and phosphate release by PAOs) and aerobic conditions (nitrification and phosphate uptake by PAOs) in each reactor (Fig. 4b). Thus, this strategy provides the following advantages: 1) alternating redox conditions enabling EBPR in the same reactor, 2) combining N-removal and EBPR in a continuous flow MBBR without the need of buffer volumes and 3)

maximum utilization of internal carbon for nutrient removal without any recirculation streams.

To avoid discharging effluent with high phosphate and ammonium concentrations, the effluent was extracted from the reactor with the lowest concentrations. To ensure reasonable concentration variations, and to avoid too many phase-shifts, the full operational cycle lasted for 2.5–3 h, and each phase length was adjusted over time to obtain the conditions required for the targeted biological processes and varying operation strategies. The time distribution between aerated and unaerated conditions changed during the different operational periods to meet varying load and removal rates (Table 1). These adjustments were either applied manually, with fixed times for each phase, or automatically. With automatic phase control, the transition from one phase to the other was made based on a fulfilled transition criterion, where online measurements on NH_4^+-N and NO_X^--N were compared to setpoints to determine when nitrification and denitrification targets were achieved, within set time limitations (max/min).

2.4. VFA dosage

The VFA was dosed to the reactor receiving the influent wastewater. A mixture of acetate (26% as COD) propionate (41%) and butyrate (33%) was added, mimicking the addition of fermentate from filter primary sludge fermentation at 5 d hydraulic retention time (HRT) and ambient temperature [24,25]. The VFA dose was adjusted weekly to the wastewater temperature, based on the VFA-COD dose (mg COD/L influent wastewater) according to Eq. (1), where $VFA_{20} = 43.4$ mg COD/L and $\Theta = 1.099$, with the exception of period E (see Section 2.5), when a higher dose was applied to evaluate the effect of having more available VFA. Fig. S6 displays the actual VFA dose during the study, together with the calculated theoretical VFA dose according to Eq. (1).

$$VFA = VFA_{20} \bullet \theta^{(T-20^\circ C)} \quad (1)$$

2.5. Operation and experimental periods

The study started August 30, 2023, and lasted for 470 days. The influent wastewater composition and the hydraulic load to the pilot plant differed over time, the latter due to changes in influent flow to the main WWTP (Table 1). The normal range of HRT was 12–17 h, and reactor temperatures varied between 12 and 25 °C (Table 1, Fig. S1b). The COD loading rate was in the range of 0.4–0.8 kg/(m^3, d), including the VFA addition (Fig. S1c). The operational periods of the study were characterized by different modes of cycle control and different strategies for VFA dosage (Table 1).

During the startup (period A), the influent wastewater to the biofilm reactors was filtered through the 1000 μm drum filter only, for the first 22 days. Thereafter, the RBF and the VFA addition were in operation until the end of period F. The priority during the start-up period was to promote EBPR rather than nitrogen removal, by applying a relatively high load to the system. During periods A to C, the flow rate to the pilot, and hence the HRT, was fixed. Thereafter, the flow rate was proportional to the main WWTP influent, resulting in varying HRT both during the day and between days (Fig. S1a).

During periods A-C, VFA was dosed at a constant rate to the reactor receiving the influent under both anoxic and anaerobic conditions (Table 1). In periods D and E, VFA dosage to the anaerobic phase was implemented, which was determined based on redox measurements (low nitrate concentrations = low redox). The redox setpoint for starting the dosage varied in the range of −60 to 50 mV. During and after heavy rains, redox in the reactors was higher and the setpoint was increased. In practice, the redox-based control meant that the VFA was dosed about half to one third of the cycle time at a rate two or three times the daily average rate (Fig. S2). During period F, the effect of the two different VFA dosing strategies was assessed by switching between the two methods. The VFA dosing was stopped day at 460.

2.6. Sampling

Flow proportional 24-h samples were collected from the influent and effluent three days per week (00:00–24:00 on Sundays, Tuesdays and Thursdays) with automatic samplers 1027 (Bühler). In addition, grab samples were taken regularly to monitor the online analysers. The automated samplers withdrew settled effluent from a sediment trap in periods A and B. In period C and onwards, effluent was collected from a separate sampling bucket to properly include the particulate fractions in the effluent. From day 300, effluent samples of soluble compounds were taken from the upper phase of the sampling bucket to avoid a slight overestimation of phosphate (see Supplementary material).

Stereoscopy was used to follow the size and appearance of the support material with biofilm development over time. To quantify the support material with biofilm in the reactors, the bed volume was measured on a daily to weekly basis. The bed volume in the reactors was defined as the volume fraction (%) of the support material (including biofilm) after ~30 s of settling in a 1-L cylinder with reactor content, sampled from 0.4 m reactor depth during aeration.

2.7. Batch tests for phosphate release and uptake

Three types of batch tests were conducted to study the activity of PAOs: 1) phosphate release after acetic acid addition, 2) phosphate uptake at anoxic and aerobic conditions, and 3) assessment of VFA dosage to the anoxic or anaerobic phase. For all tests, 2.5 L of the reactor content (biofilm support material and water) was collected from the reactors, the biofilm support material was washed and transferred to separate batch test reactors with inorganic nutrient medium for a test volume of 2.5 L. For details about the batch tests, see the supplementary material.

2.7.1. Phosphate release

Phosphate release from the biofilm biomass was induced by adding sodium acetate (150 mg COD/L) at anaerobic (DO <0.3 mg O_2/L) conditions, constant pH (7.2) and temperature (20 °C). The test lasted for 2 h.

2.7.2. Phosphate release and uptake at aerobic and anoxic conditions

Phosphate release was conducted in one batch test reactor as above (2.7.1), but with addition of VFA (2.4) at a concentration of 150 mg COD/L. Thereafter, the reactor content was transferred to two batch test reactors and supplied with excess phosphate (60 mg PO_4-P/L). In the two reactors, phosphate uptake was studied for 2 h at aerobic and anoxic conditions, respectively.

2.7.3. VFA dosage at anoxic and anaerobic conditions

Two batch test reactors with biofilm biomass were subjected to anoxic conditions (1.5 h) followed by anaerobic conditions (1.5 h). In one of the reactors, VFA (see 2.4) was added in the anoxic period and in the other reactor, VFA was added in the anaerobic period. VFA was added at concentrations corresponding to in the pilot reactor (29 mg COD/L). In both reactors, the turnover of nitrate and phosphate was measured as indications of denitrification and EBPR activity.

2.8. Analyses and calculations

Composite samples from the pilot plant and samples from batch tests were filtered through 1.6 μm MGA Munktell glass fibre filters (Ahlström Munksjö) for analysis of PO_4^{3-}-P, NH_4^+-N, NO_2^--N and NO_3^--N by calorimetric method with Gallery Plus (Thermo Scientific) according to ISO 15923-1:2013 and for analysis of soluble COD. P_{tot}, N_{tot} and COD were measured with cuvettes LCK 349/350, LCK138/238 and LCK 814/1814 (Hach). TSS and VSS were analysed according to standard methods (SS-EN 872, 2nd ed. and SS 028112, 3rd ed., respectively).

Since the suspended biomass was included in the effluent sample, the

removal efficiencies of nitrogen and phosphorus were calculated assuming separation of the particulate fraction in subsequent post-treatment (Eqs. (2) and (3)).

$$N_{red} = \frac{[N_{tot}]_{in} - [NH_4^+ - N]_{out} - [NO_2^- - N]_{out} - [NO_3^- - N]_{out}}{[N_{tot}]_{in}} \quad (2)$$

$$P_{red} = \frac{[P_{tot}]_{in} - [PO_4^{3-} - P]_{out}}{[P_{tot}]_{in}} \quad (3)$$

Assimilated phosphorus was calculated from the effluent particulate COD, with a conversion factor of 0.010 g P/g COD typical for heterotrophic bacteria [27]. Phosphorus removal by EBPR was calculated as the difference between effluent particulate phosphorus and assimilated phosphorus.

2.9. Microbial community analysis

Support material with biofilm was collected from the bed volume assessments for microscopy (weekly) and for DNA analysis (monthly). DNA was extracted using the FastDNA Spin kit for Soil (MP Biomedicals) according to the manufacturer's recommendations. PCR amplification of the SSU rRNA gene was carried out with the primers 515FB and 1391R [28,29]. The library of amplicons was sequenced using the Oxford Nanopore Technology in a PromethION R10.4.1 flowcell towards the MinKNOW 24.02.10 software. The sequencing reads were mapped against the SILVA 16S/18S rRNA 138 SSURef NR99 full-length database curated for *Ca.* Phosphoribacter and *Tetrasphaera* separation. Bioinformatic processing was conducted in R (4.4.1). Raw sequence reads are deposited in the Sequence Read Archive (SRA), NCBI, Bioproject: PRJNA1279609. For details about the workflow and bioinformatics, see the supplementary material.

3. Results and discussion

3.1. Biofilm development and start-up

Biofilm began to colonise the support material from the first weeks of operation (Fig. 2a). The amount of biofilm, as measured by the bed volume, varied quite significantly during the first 280 days (periods A-D, Fig. 2c). During initial colonization, the bed volume increased sharply, and fluffy biofilm with ciliates could be observed by stereoscopy on day 45 (Fig. 2a). The bed volume dropped due to loss of support material on day 90 (see Supplementary material), but once the lost material was replaced, the bed volume recovered despite low winter temperatures (Fig. 2c). The peak in bed volume around day 200 (Fig. 2c) might be explained by the feathery biofilm at the time (Fig. S3). The biofilm seemed denser after 300 days of operation, although ciliates still grew out from the biofilm (Fig. S3). Both bed volume and biofilm appearance

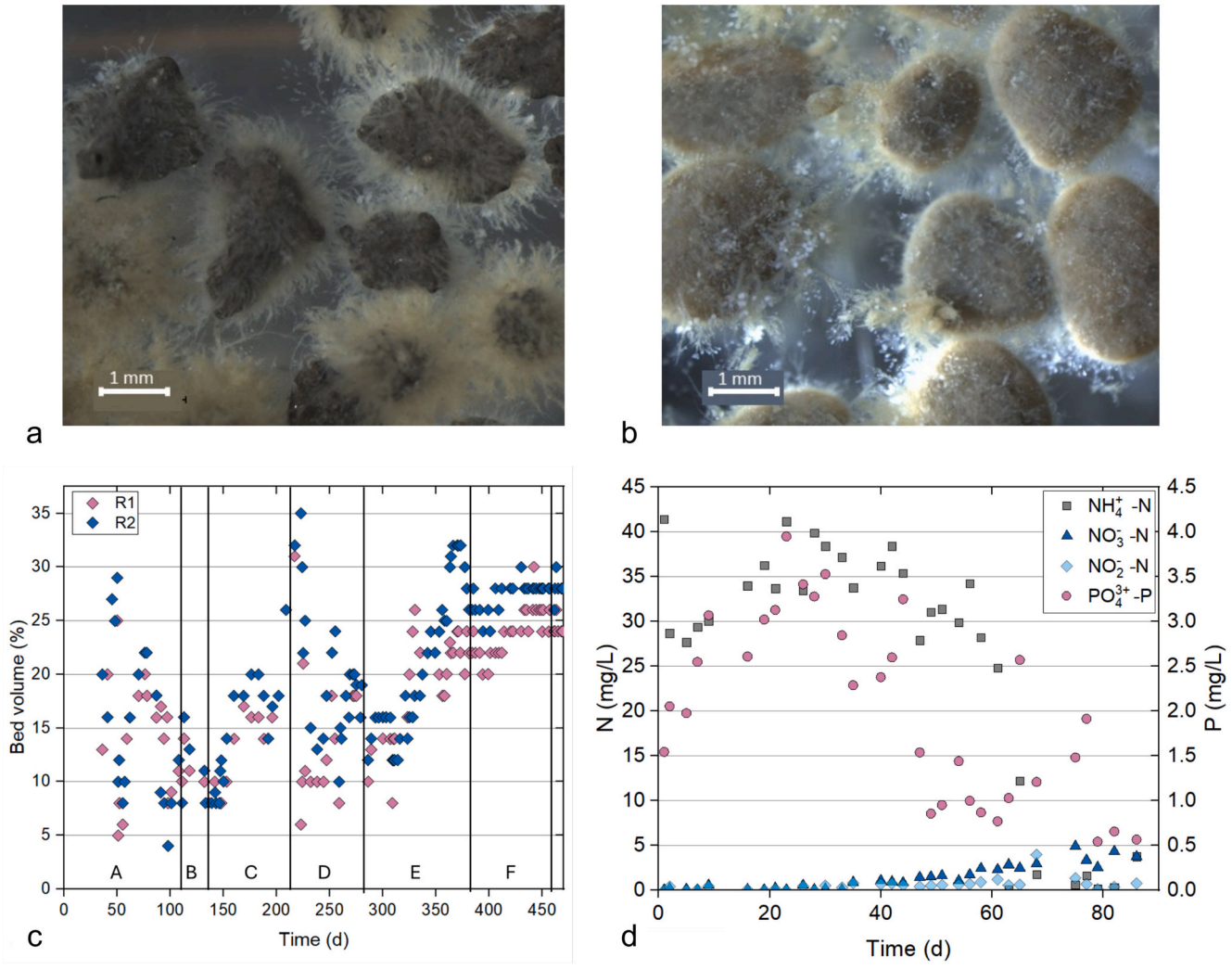

Fig. 2. Support material with biofilm a) day 45 and b) day 406. c) Bed volume in R1 and R2. d) Effluent concentrations of ammonium, nitrite, nitrate and phosphate in 24-h composite samples during the start-up (period A).

were stable thereafter, with a dense and more uniform biofilm during period E and F (Fig. 2b, Fig. S3). During the course of the study, no degradation of the support material was observed by stereoscopy or bed volume assessments.

As biofilm colonised the support material, the concentration of phosphate in the effluent decreased after 40 days of operation, and at the same time nitrification was observed as nitrate and nitrite production (Fig. 2d). After a gradual increase in HRT until day 48, nitrification improved with sharply decreased effluent ammonium levels. After 80 days of operation, effluent phosphate and nitrogen indicated enhanced nutrient removal (Fig. 2d), showing that the strategy of applying an initially high and gradually decreasing load during start-up (Fig. S1) was successful for process establishment. The 11 weeks start-up period was similar to previously reported 12 weeks in studies of other biofilm EBPR processes [10,30,31]. In this study, nitrogen removal was also achieved within the start-up time, which has not yet been shown for a biofilm EBPR processes. Following the start-up, several technical issues during period B—D led to process disturbances as well as temporal losses of support material through the separators. Although it is interesting to observe how the system responded to the many disturbances in the pilot operation during period B—D, stable process performance is only assessed for period *E*-F.

3.2. Microbial community composition

In the two reactors, the succession of the microbial communities followed the same pattern indicating no preferential selection in the two reactors (Fig. S4). Heterotrophic bacteria within Psedumonadota, like *Acidovorax*, *Pseudorhodobacter*, and *Acinetobacter* were initially abundant in the biofilm but quickly decreased in abundance as the biofilm established (Fig. S5a). Similar patterns of rapid rise in heterotrophic bacteria within Pseudomonadota followed by washout have been shown in other wastewater biofilms, suggesting a role of these bacteria as early colonisers [32]. Microorganisms related to nitrification were observed day 87 when ammonia-oxidising bacteria (AOB) within *Nitrosomonas*, nitrite-oxidising bacteria (NOB) within *Nitrotoga* and nitrite- or complete ammonia-oxidising *Nitrospira* appeared (Fig. 3a). At this time, operational data clearly showed ongoing nitrification (Fig. 2d). *Nitrotoga* was the most abundant nitrifier until day 273, after which, during the warmer summer months, the relative abundance of *Nitrospira* increased to more than 10% relative abundance among identified operational taxonomic units (OTUs). This increase coincided with a decreasing relative abundance of *Nitrotoga*. The shift from *Nitrotoga* to *Nitrospira* during the warmer months was likely a result of lower temperature preferences of *Nitrotoga*, as previously observed by their distribution in WWTPs [33] and coculture experiments [34]. The relative abundance of *Nitrosomonas* was more stable and slowly increasing over time to around 2% (Fig. 3a).

Several groups of PAOs were found in the biofilm, which supports the presence of EBPR in the process. The most abundant PAO in the biofilm were *Tetrasphaera* and *Ca.* Phosphoribacter, formerly classified within *Tetrasphaera* [35]. *Ca.* Phosphoribacter has commonly been detected in WWTPs worldwide [35,36], and has recently been found at high abundance in a biofilm EBPR reactor [37]. In this study, *Ca.* Phosphoribacter and *Tetrasphaera* were both observed at rather high relative abundances (3–8%) of identified microorganisms already day 45 (Fig. 3b), concomitant with the decrease in the effluent phosphate concentrations (Fig. 2d). After start-up, *Tetrasphaera* gradually decreased, while *Ca.* Phosphoribacter fluctuated at higher relative abundances until period E, when they also declined (Fig. 3b). An opposite pattern was observed for *Ca.* Accumulibacter, which was most abundant in the later periods (Fig. 3b). Potentially phosphate-accumulating *Thiothrix* [38] was represented by several species and varied over time (Fig. 3c, Fig. S5b). The shift in composition of PAOs from day 273 onwards, with an increasing fraction of *Ca.* Accumulibacter and decreasing fractions of *Ca.* Phosphoribacter and *Tetrasphaera* was likely related with a higher VFA dose in this period (Fig. S6), since *Ca.* Accumulibacter are dependent on VFAs, while *Tetrasphaera* and *Ca.* Phosphoribacter can use fermentable carbon sources [39,40]. However, the total relative abundance of PAOs in the biofilm declined considerably in relative abundance day 280 onwards despite high PAO activity (see 3.4.2). Furthermore, the relative abundance of PAOs in the effluent was low in this period (Fig. S5b) despite functional EBPR (see 3.4.3). Hence, we cannot exclude the possibility that other undetected PAOs were present in the biofilm and contributed to the EBPR.

The GAO *Ca.* Competibacter was abundant in the biofilm and increased during period E, at higher temperature and VFA dose (Fig. 3c). *Ca.* Competibacter is increasingly competitive for VFA at higher temperatures, as opposed to *Ca.* Accumulibacter [36,41], which could explain the increase in *Ca.* Competibacter and concomitant decrease in *Ca.* Accumulibacter after day 300.

When comparing the microbial composition in the effluent to that in the biofilm (Fig. S5b), it is noticeable that no nitrifiers were detected in the effluent, suggesting negligeable detachment. However, *Ca.* Phosphoribacter, *Tetrasphaera* and *Thiothrix* were detected in the effluent, indicating a continuous detachment of PAOs from the biofilm, which is essential to obtain EBPR. No spatial analysis was made of the different microbial groups in the biofilms, but the findings suggest that the nitrifiers were growing in deeper biofilm layers, with the faster growing heterotrophic organisms located at the surface of the biofilm and thus exposed to higher shear forces.

To summarise, multiple clades within the key functional groups of nitrifiers, PAOs and GAOs were identified the biofilm, with dynamics over time in abundances, presumably driven by shifts in temperature and availability of readily biodegradable organic carbon.

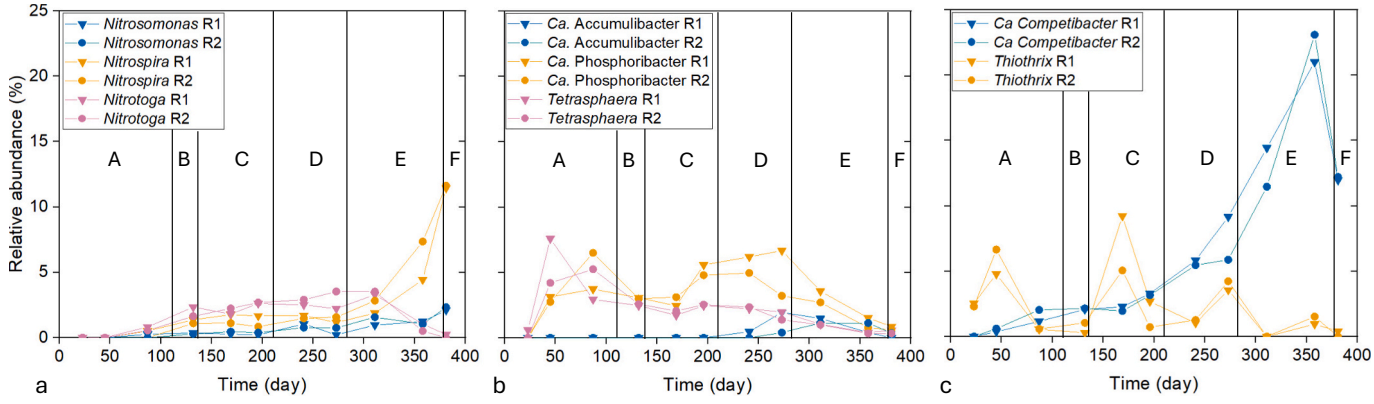

Fig. 3. Relative abundancies of identified OTUs aggregated at genus level of a) nitrifying bacteria, b) known PAOs, c) GAOs and putative PAOs.

3.3. Nitrogen removal

The aim of this study was to obtain EBPR while also achieving efficient nitrogen removal (>80% based on effluent TIN). Following the start-up, an effluent total inorganic nitrogen (TIN) of <10 mg N/L was reached during the major part of the study (Table 2). High nitrogen removal was achieved during period B, where automatic phase control was applied to optimise the performance. In periods C—D, however, the HRT was somewhat decreased, which, in combination with lower temperatures (Fig. S6), technical disturbances (see Supplementary material), and suboptimal settings of the automatic phase control, led to discharge of water with higher TIN concentrations (Tables 1–2). During periods E and F, the HRT was increased and the system was operated with fixed cycle phase times, resulting in improved and stable nitrogen removal with effluent concentrations of 5.5 ± 2.4 and 5.3 ± 1.0 mg NO_3^--N/L, 1.0 ± 0.8 and 2.2 ± 2.6 mg NH_4^+-N/L, and 6.9 ± 2.3 and 7.9 ± 2.7 mg TIN/L, during periods E and F, respectively (Table 2, Fig. S7a). The corresponding nitrogen removal of around 85% (Table 2) was maintained within the applied loading rate of 50–105 g N/(m^3, d) in periods E-F (Fig. 7a). The aim to achieve efficient nitrogen removal with >80% removal was reached. Furthermore, the results imply that the maximum loading rate regarding nitrogen removal can be higher than in this study, which is positive for full-scale implementations. For comparison of the obtained nitrogen removal with other biofilm EBPR processes, see Section 3.5.

In the typical pattern over a reactor cycle measured online (Fig. 4b), the ammonium concentration increased during the non-aerated phases due to the influent ammonium, and decreased during the aerated phases, while the nitrate and nitrite concentrations displayed the opposite pattern. Ammonium removal was typically faster than nitrate removal (Fig. 4b), indicating that denitrification rather than nitrification was the rate-limiting step for the overall nitrogen removal. Hence, online data of momentary nitrification and denitrification rates can assist in further optimization of the nitrogen removal. Since the focus of this study was the phosphorus removal, this remains to be done.

3.4. Phosphorus removal

Following the drop in effluent phosphate concentrations during the start-up (Fig. 2d), EBPR activity was observed in the system throughout the operational period, in the cyclic phosphorus dynamics (*i.e.* Fig. 4b), as well as in separate batch tests (Figs. 5 and 7).

3.4.1. Phosphate release

The phosphate release batch tests, using acetate as carbon source, showed similar rates between the two reactors throughout the operational period, with a few exceptions where R1 had a higher release rate (Fig. 5a). The observed phosphate release was around 10 mg PO_4^{3-}-P/L during period B—C, after which it increased gradually, reaching as high as 40 mg PO_4^{3-}-P/L during phase E and F (Fig. 5a). The phosphate concentrations in batch tests of phosphate release were in the same range as other experiments with MBBRs [8] [11,42].

Interestingly, the increase in phosphate release in periods E-F coincided with the decline in relative abundance of PAOs as observed in the microbial analysis (Fig. 3b). The total amount of biomass in the reactors as measured by the bed volume was, however, increasing during this period (Fig. 2c), suggesting that the total amount of PAOs was still sufficient to maintain EBPR. It is also a possibility that other undetected PAOs were present in the biofilm and contributed to the EBPR. The high abundance of GAOs during this time (Fig. 3c) did not seem to have a detrimental effect of the EBPR activity.

The ratio between phosphate release and COD uptake in the trials also increased continuously over time, from 0.1 to 0.4–0.5 g P/g COD. The gradual increase was interrupted with a period when the ratio was stable around 0.3 g P/g COD during days 300–350 (Fig. 5b) at high VFA dose and high temperature (Fig. S6). The phosphorous release to COD uptake has been shown to decrease at higher loading of carbon source [11,43], which is in line with this observed drop during higher VFA addition. VFA uptake by GAO likely occurred during this time, as it coincides with the increase in *Ca.* Competibacter relative abundance (Fig. 3c), and would explain the moderate PO_4^{3-}/COD ratio [43–45]. It should however be noted that the ratios during the later periods (Fig. 5b) are comparable to those of other biofilm systems of 0.2–0.5 mg P/mg SCOD for SBBR [4], 0.23 for fixed biofilm [30] and 0.39 for continuous AGS [46].

Separate batch tests were conducted to study the impact of VFA dosage on phosphate release and denitrification for helping in assessing how the VFA would be of best use in the MBBR operation. VFA was added to the anoxic phase in one batch reactor and to the anaerobic phase in another batch reactor. The tests demonstrated that when VFA was added to the anoxic phase, denitrification was faster, but the difference in nitrate consumption at the end of the test was minor for the two VFA dosage strategies (Fig. S8). The phosphate release, on the other hand, was profoundly affected by the VFA dosing strategy. Adding the VFA to the anaerobic phase resulted in a phosphate release of 8–10 mg PO_4^{3-}-P/L, while VFA addition in the anoxic phase resulted in much smaller release of 2–3 mg PO_4^{3-}-P/L. The phosphate release in the anoxic phase may be explained by anaerobic conditions in the deeper biofilm layers, but also by activity of non-denitrifying PAOs which may take up VFA as under anaerobic conditions [47]. It is likely that such non-denitrifying PAOs would be favoured by adding VFA continuously compared to by adding VFA during anaerobic conditions.

3.4.2. Phosphate uptake

Batch tests demonstrated phosphate uptake under both aerobic and anoxic conditions (Fig. 6). Over time, there was a gradual increase in the aerobic phosphate uptake, while the anoxic uptake was more variable and lower, especially after the summer period at days 364 and 448 (Fig. 6c-d).

Although the aerobic phosphate uptake was higher, the anoxic uptake rate was considerable. The ratio between the anoxic and aerobic uptake rate after 2 h was between 0.39 and 0.87, similar to the 0.58 previously measured for MBBR [8] and higher than the 0.13–0.46 previously measured in full-scale plants with activated sludge [48]. The results support that the biofilm process with addition of VFAs, representing fermentate from filter primary sludge, promoted denitrifying PAO activity. Indeed, biofilm growth mode has recently been employed in reactors aiming for enriching denitrifying PAOs [49]. In the pilot reactors, inflow of phosphate occurred in the anoxic phase, allowing for denitrifying PAOs to replenish their polyphosphate storage. The difference observed over time with respect to the anoxic phosphate uptake

Table 2
Average effluent concentrations and removal efficiency (Eq. 2, 3) for the biofilm pilot plant during the different operational periods after the start-up (mean ± standard deviation).

Period	B	C	D	E	F
Day	112–135	136–211	211–279	280–380	381–460
Number of samples	8	26	23	37	31
N load (g/(m^3,d))	61 ± 15	79 ± 24	84 ± 19	80 ± 13	80 ± 14
N removal efficiency (%)	81 ± 6	70 ± 10	72 ± 10	85 ± 5	84 ± 5
NH_4^+ (mg N/L)	2.2 ± 2.3	8.2 ± 5.6	6.5 ± 5.2	1.0 ± 0.8	2.2 ± 2.6
NO_2^- (mg N/L)	0.3 ± 0.1	0.4 ± 0.1	0.5 ± 0.2	0.4 ± 0.1	0.4 ± 0.1
NO_3^- (mg N/L)	4.0 ± 1.6	3.2 ± 1.2	4.8 ± 2.1	5.5 ± 2.4	5.3 ± 1.0
TIN (mg N/L)	6.6 ± 3.2	11.7 ± 5.1	11.7 ± 4.0	6.9 ± 2.3	7.9 ± 2.7
PO_4^{3-} (mg P/L)	0.8 ± 0.4	1.3 ± 0.5	2.3 ± 1.1	1.8 ± 1.3	1.8 ± 1.0
P removal efficiency (%)	82 ± 12	68 ± 15	57 ± 18	67 ± 23	68 ± 18

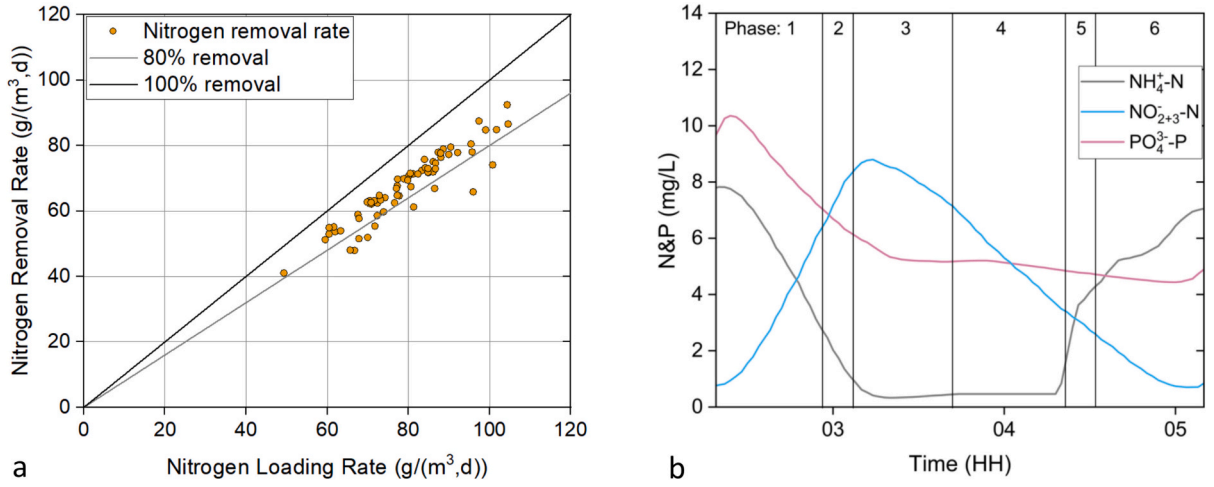

Fig. 4. a) Nitrogen removal rate *versus* nitrogen loading rate during periods E-F, with 100% and 80% nitrogen removal marked as references. b) Typical concentration dynamics over one reactor cycle (Phases 1–6), as measured online in R2 on day 439, (note that effluent was discharged from R2 during phases 2–4).

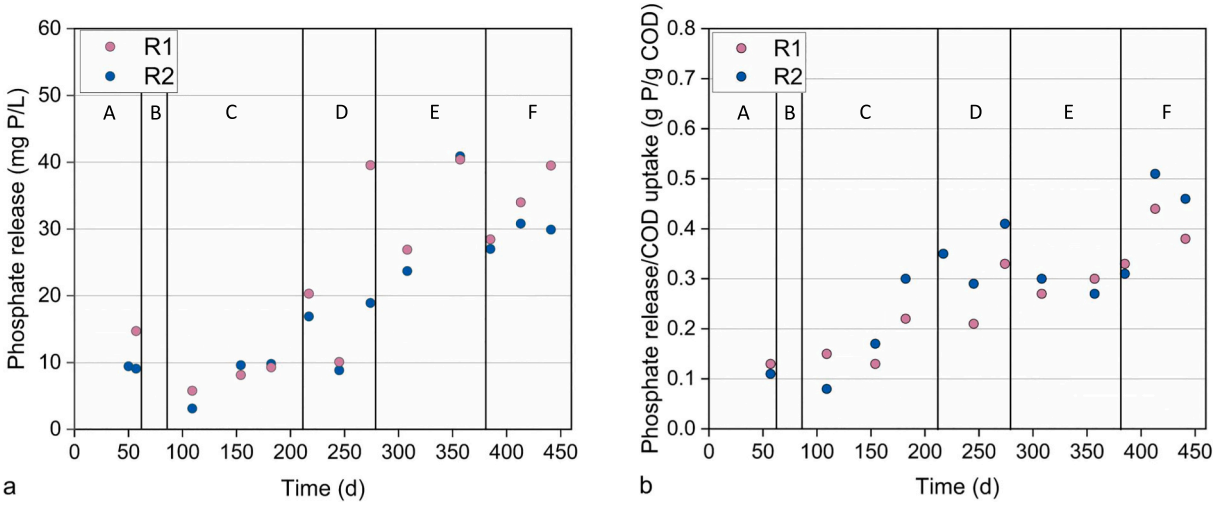

Fig. 5. Batch tests with biofilm from R1 and R2 showing a) Phosphate release after 1.5 h. b) Ratios between phosphate release and COD uptake after 1.5 h.

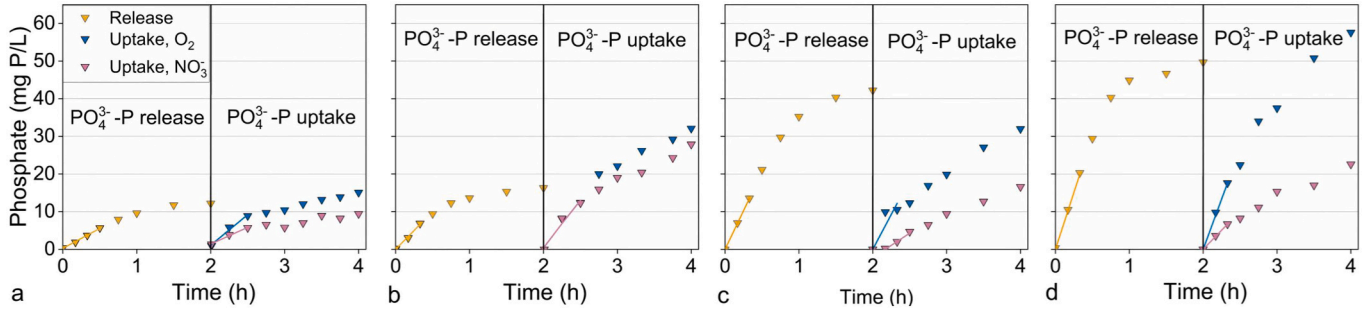

Fig. 6. Batch tests showing phosphate release (yellow) followed by phosphate uptake at aerobic (blue) or anoxic (pink) conditions. Solid lines indicate the rates of release and uptake during the first half hour. a) Day 78. b) 9 Day 192. c) Day 364. d) Day 448. (For interpretation of the references to colour in this figure legend, the reader is referred to the web version of this article.)

was likely caused by seasonal variations and the change in VFA dose, and presumably also by changes in the composition of PAOs.

Many members of *Ca.* Phosphoribacter and *Tetrasphaera*, which were abundant in the biofilms, possess genes to use both nitrate and nitrite as electron acceptor [39]. Anoxic phosphate uptake has been measured in activated sludge alternating flow reactors and SBR with high fractions of *Ca.* Phosphoribacter and/or *Tetrasphaera* [48,50]. Due to the differences in abilities even between closely related PAOs [39,51], it is, however, not possible to fully relate the microbial composition to the capacity for anoxic phosphate uptake.

3.4.3. EBPR reactor performance

When studying the system performance, the overall phosphorus removal efficiency as well as the estimated EBPR of the system varied over time, as the reactor conditions and operation strategies varied (Fig. S7b, c). Below, EBPR reactor performance is assessed for periods *E-F*, when operation was stable (see Section 3.1).

The VFA dose had strong influence on the phosphorus removal efficiency, which was clearly shown in period E when VFA was dosed at various levels during relatively stable temperature (Fig. 7a). With a VFA dose of 25–55 mg COD/L, corresponding to the predicted VFA production from fermentation of primary sludge, phosphorus removal was 40–80%, while removal was lower, down to 20%, during heavy rainfall and lower VFA dose. A dose of >100 mg COD/L was needed to reach over 90% phosphorus removal (Fig. 7a). During period F, when the VFA dosage corresponded to the predicted VFA production and the dosage was based on redox, the average phosphorus removal in the pilot reactors was 68 ± 18% with corresponding effluent phosphate concentrations of 1.8 ± 1.0 mg P/L (Table 2).

Due to the wastewater primary filtration, ratios of total- and soluble COD/P in the influent wastewater were low, at 53 and 20 g/g, respectively (period F). With VFA addition, these ratios increased to 60 and 28 g of total- and soluble COD/g P, respectively. The influent wastewater COD/P ratio is an influential parameter for EBPR [52]. It has been estimated that 20 g VFA-COD is required to remove 1 g of P [27]. The soluble COD to P_{tot} ratio of 20 g COD/g P in this study is thus low if carbon source from degraded particles is not available, due to the lack of readily biodegradable carbon source. It is therefore not surprising that VFA dosing had a strong influence on the EBPR in the reactors.

The EBPR process relies on the extraction of phosphorous-rich biomass from the bioreactor. A linear correlation could be observed between the calculated EBPR (assimilation subtracted) and the phosphorus to COD ratio of the particles detaching from the biofilm and ending up in the effluent (Fig. 7b). The phosphorus to COD ratio of the effluent particles increased from 0.01 to 0.03 as the phosphorus removal increased, which strongly suggests that detachment of phosphorous-rich biomass from the biofilm in the continuous MBBR supported EBPR.

3.4.4. Redox control of VFA dosage

The impact of redox control for the VFA dosage was evaluated in the pilot plant during period F, by periodically switching between having a constant VFA dosing and an intermittent, redox-based VFA dosing. The redox-based VFA dosing resulted in a daily pattern of lower phosphate concentration during daytime, and higher peaks during evenings and nights (Fig. S2). Effluent withdrawal was avoided from the reactors during such peaks by the phase control (Fig. 1).

Fig. 8 displays the dynamics in R2 during this period, with the highest (peak) and lowest (low) observed nitrate plus nitrite and phosphate concentrations for each operational cycle. The low phosphate value corresponds to the concentrations when effluent was discharged, whereas the peak values indicate the phosphate release and hence the PAO activity. The periods with redox control were characterized by higher phosphate peaks as well as lower phosphate concentration during the aerated phases, indicating an elevated PAO activity (Fig. 8b, d). The mean difference in peak- and low values with redox control and constant dosing (days 401–437) were 3.5 ± 2.3 mg PO_4^{3-}-P/L, and 2.3 ± 1.2 mg PO_4^{3-}-P/L, respectively, with a significant difference ($P < 0.0001$) of 0.6 mg/L (Fig. 8d, Table S2). The corresponding values for the low phosphate concentrations were also significantly different ($P < 0.0001$) at 1.8 ± 1.2 mg PO_4^{3-}-P/L with redox control and 2.4 ± 0.9 mg PO_4^{3-}-P/L with constant dosing (Fig. 8). At day 460, the VFA dosing was turned off completely, which led to an increase in effluent phosphate, and a diminished difference between peaks and low values (Fig. 8b).

The effect of VFA control strategy on denitrification was negligible (Fig. 8a, c). During day 401–428, the low values for nitrate during redox and constant VFA dosing were similar at 1.9 ± 0.6 and 1.9 ± 0.4 mg NO_{2+3}^{-} -N/L, respectively, with no significant difference ($P = 0.53$). Based on these results, redox-based VFA dosage to the process is recommended to favour EBPR without compromising denitrification.

3.5. Overall process performance

There are relatively few studies of EBPR and nitrogen removal in MBBRs with municipal wastewater, but the results from this study of 84% and 68% removal of nitrogen and phosphorus, respectively, with a mean VFA addition of 47 mg COD/L (Table 2, period F), can be compared to 54 and 75% removal with 80 mg COD/L acetate added [11] and 20 and 81% with 50 mg COD/L of acetate (Table S3) [4]. Nitrogen and phosphorus removal of 70% and 68% [53], and 70% and 86% [42] has been achieved without VFA addition (Table S3). Since nitrogen and phosphorus removal occur at the expense of each other in the reactor operation, it is difficult to achieve high removal of both. In this study, high nitrogen removal has been a prerequisite, and higher phosphorus removal could probably be attained at the expense of higher effluent nitrogen concentrations or lower volumetric productivity. Overall, it seems that a continuous MBBR, as tested in this study, may reach similar levels of removal efficiencies for nitrogen and phosphorus as SBBRs (Table S3) without the need for additional volumes for flow equalisation.

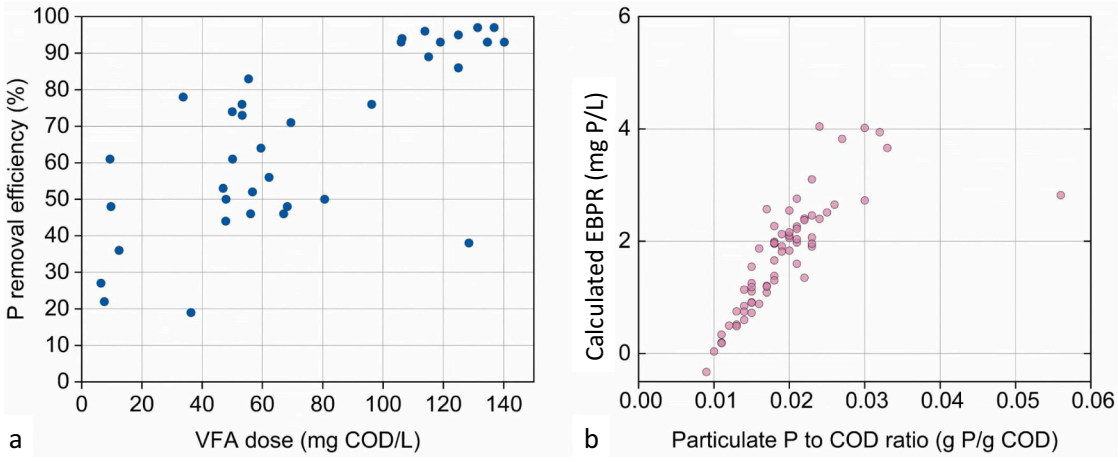

Fig. 7. a) Phosphorus removal efficiency (Eq. (3)) *versus* VFA dose in period E. b) Calculated EBPR (difference between effluent particulate and assimilated phosphorus) *versus* the ratio of phosphorus to COD in effluent particles in periods E-F.

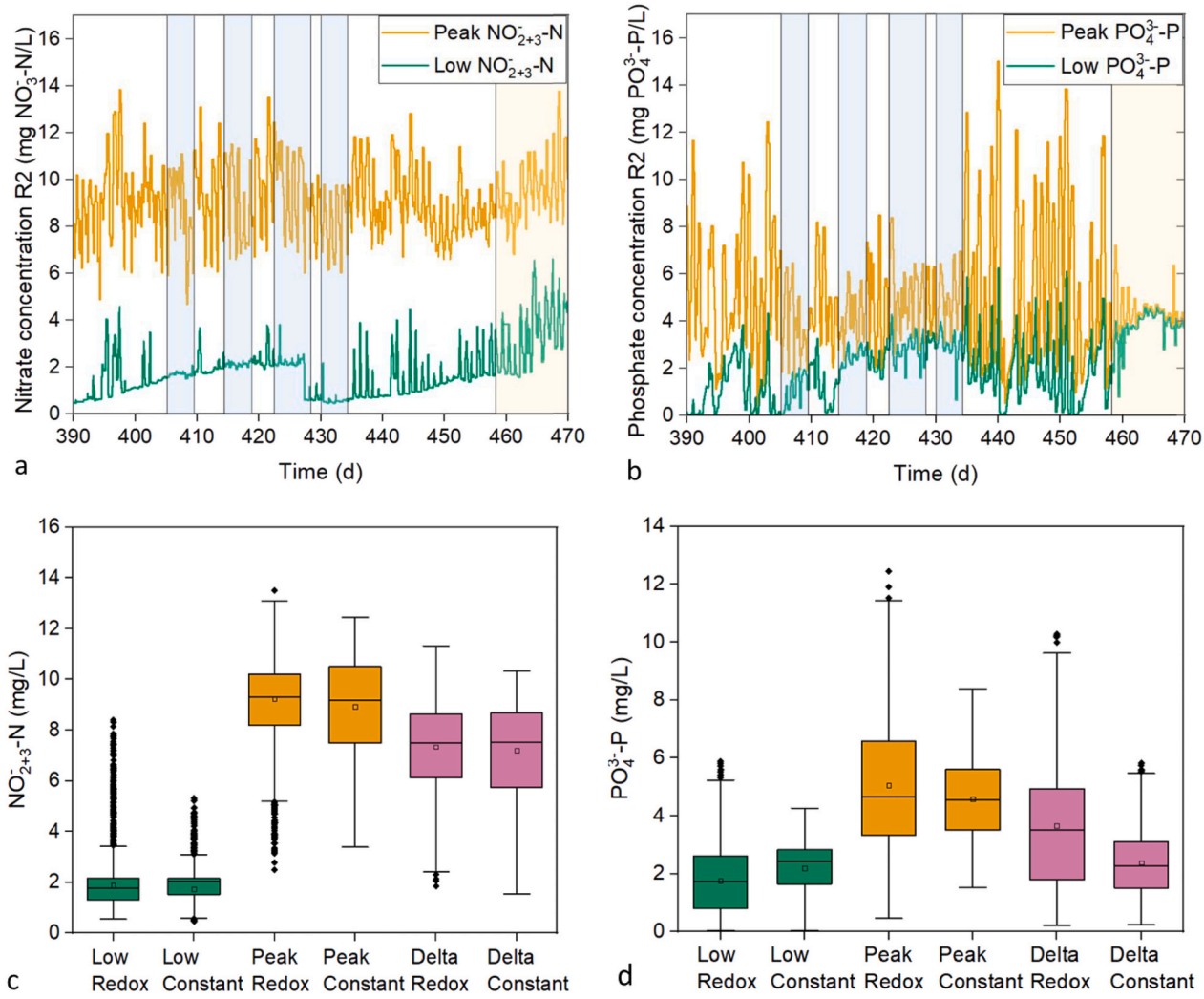

Fig. 8. Variations in online analysis of a) nitrite plus nitrate and b) phosphate, during intermittent periods of VFA dosing based on redox (white) and constant dosing (blue), and no dosing (yellow). The nitrate+nitrite sensor was calibrated on day 427. The low values during each cycle (aerated phases) are in green, and the peak values (unaerated phases) are in orange. Boxplots of low and peak values as well as their difference (delta) with redox and constant VFA dosing are shown for c) nitrite plus nitrate, d) phosphate. (For interpretation of the references to colour in this figure legend, the reader is referred to the web version of this article.)

3.6. *Prospects for optimization and full-scale implementation*

This study is the first demonstration of how efficient nitrogen removal combined with EBPR could be achieved in a continuous MBBR system, with alternating flow and carbon management by primary sludge fermentation. This system could thus be a more compact alternative to conventional processes for nutrient removal, without the need for sludge recycling, resulting in an improved energy recovery potential, and no need for buffer volumes or recirculation pumps. But although the performance seems to be in parity with previous observations of compact systems, there are aspects to consider for future optimization and full-scale implementation.

During most part of this study, the cycle phase lengths was kept constant in order to minimise the number of variables for observability and the automatic phase control was not optimised. A more optimised automatic cycle control, with fine-tuned phase-transition criteria based on online variables or manipulations thereof, could potentially improve the process efficiency and effluent values, and is currently under development.

VFA addition, mimicking fermentate addition, was shown to be an advantageous approach to address the dependency on influent COD in MBBRs. The impact of fermentate addition could however differ in a real installation. For example, solubilised phosphate from the fermentation would be added with the carbon source in the order of 0.016 mg P/mg soluble COD [24]. On the other hand, only the VFA-COD was added in this study, although the fermented sludge soluble COD contained on average 77% VFA [24]. For every mg COD of VFA added to the wastewater, another 0.3 mg of COD would be added as soluble non-VFA COD from the fermentate. The VFA production from primary sludge may also be increased by raising the fermentation temperature, which would lead to more available VFA and a higher phosphorus removal.

Constant dosage of VFAs, as tested in this study (Fig. 8), can exemplify in-line hydrolysis in a primary settler [54], which would not enable control of the VFA addition. The redox-controlled VFA dosage in this study, or control of VFA addition based on the phosphate concentration, would be possible only with side stream fermentation with sufficient buffering volume for the fermentate. The typical VFA addition in full-scale activated sludge EBPR is with the influent, to the anaerobic zone [55] or to the anaerobic phase in SBRs such as in AGS processes [56]. Thus, adding the VFAs after the denitrification, at low redox, is in line with the applied knowledge of EBPR. The setpoint for VFA dosage was, however, not easy to optimise (Fig. S6). It is therefore recommended to apply a variable redox value depending on the flow rate and nitrate concentration to fine-tune the control.

Considering the origin of the source material, the durability of the biofilm support material is critical. This study did not show any signs of

degradation or wear of the material, which is in line with previous experiments showing the that the support material was intact after 3.5 years of operation [57]. However, bed volume and biofilm growth should be regularly monitored and a plan should be in place for adding more material over time if necessary. Based on the experiences in this study, retention of the support material in the reactors seems to be more critical than the risk for degradation. The losses of support material from the reactors occurring during this study were, however, mainly related to the small scale of the pilot, and is not representative of large-scale systems [57]. This study did not evaluate effluent particle removal, which is required after the biofilm process to separate the effluent solids. Considering the phosphorus requirements for large WWTPs, a post-treatment with coagulation may be needed, which would further decrease the effluent phosphate concentration. In this case, the EBPR would contribute to decreasing the coagulant dose.

4. Conclusions

The novel process was demonstrated to be a successful way to combine EBPR with high nitrogen removal in MBBRs through continuous flow with alternating reactors, use of new bio-based support material, and carbon management by primary filtration and VFA dosage. EBPR was evident from the extent of phosphorus removal in relation to organic matter, and the presence of known PAOs in the biofilm (*Ca.* Phosphoribacter, *Tetrasphaera*, and *Ca.* Accumulibacter). The alternating flow direction and intermittent aeration facilitated EBPR without moving the support material between anaerobic and anoxic/aerobic conditions and allowed directing VFAs to anaerobic uptake by PAOs. High nitrogen removal of 84 ± 5% and phosphorus removal of 68 ± 18% were observed. Denitrifying PAO activity could be shown in batch tests, indicating that anoxic phosphate removal was occurring during the entire study. Addition of VFA had a strong impact on the EBPR and dosage of VFA at low redox improved EBPR and resulted in less phosphate in the effluent, compared to constant VFA dosing, without negatively affecting the effluent nitrate level. This means that the process could favourably be combined with side stream primary sludge fermentation which allows storage and optimised dosing of internally produced VFAs. Future optimization may include automation of the reactor phase length and further development of the redox control for VFA dosage.

CRediT authorship contribution statement

E. Ossiansson: Writing – review & editing, Writing – original draft, Visualization, Methodology, Formal analysis, Conceptualization. **M. Piculell:** Writing – review & editing, Project administration, Methodology, Conceptualization. **D.J.I. Gustavsson:** Writing – review & editing, Supervision, Project administration, Methodology, Funding acquisition, Conceptualization. **S. Bengtsson:** Writing – review & editing, Supervision, Methodology, Conceptualization. **M. Christensson:** Writing – review & editing, Methodology. **C. Rosen:** Writing – review & editing, Methodology, Conceptualization. **F. Persson:** Writing – review & editing, Supervision, Methodology, Formal analysis, Conceptualization.

Declaration of competing interest

The authors declare the following financial interests/personal relationships which may be considered as potential competing interests: David Gustavsson reports financial support was provided by Sweden Water Research AB. David Gustavsson reports financial support was provided by Swedish Environmental Protection Agency. If there are other authors, they declare that they have no known competing financial interests or personal relationships that could have appeared to influence the work reported in this paper.

Data availability

Data will be made available on request.

Acknowledgements

The study was funded by Veolia Water Technologies, VA SYD and Sweden Water Research. The primary filtration pilot plant construction was partially funded by the Swedish Environmental Agency through the program City Innovations (NV-02084-18). The authors would like to acknowledge the laboratory staff (Veolia Water Technologies) for their contribution, the operational personnel (Veolia Water Technologies, Start-up and VA SYD), and Mie Bech Lukassen (DNA Sense). In addition, the authors would like to thank Sofia Lind (Veolia Water Technologies) for project management.

Appendix A. Supplementary data

Supplementary data to this article can be found online at https://doi.org/10.1016/j.jwpe.2026.110186.

References

[1] P. Izadi, P. Izadi, A. Eldyasti, Design, operation and technology configurations for enhanced biological phosphorus removal (EBPR) process: a review, Rev. Environ. Sci. Bio. 19 (2020) 561–593, https://doi.org/10.1007/s11157-020-09538-w.
[2] X. Lu, J. Zhao, H. Duan, Z. Yuan, Y. Zu, A. Oehmen, L. Ye, Exploring the feasibility of high rate enhanced biological phosphorus removal system driven by diverse carbon source, Water Res. X 28 (2025) 100365, https://doi.org/10.1016/j.wroa.2025.100365.
[3] M. Carlsson, A. Lagerkvist, F. Morgan-Sagastume, Energy balance performance of municipal wastewater treatment systems considering sludge anaerobic biodegradability and biogas utilisation routes, J. Environ. Chem. Eng. 4 (2016) 4680–4689, https://doi.org/10.1016/j.jece.2016.10.030.
[4] A.B. Fanta, A.M. Nair, S. Sægrov, S.W. Østerhus, Phosphorus removal from industrial discharge impacted municipal wastewater using sequencing batch moving bed biofilm reactor, J. Water Process Eng. 41 (2021) 102034, https://doi.org/10.1016/j.jwpe.2021.102034.
[5] H. Helness, H. Ødegaard, Biological phosphorus removal in a sequencing batch moving bed biofilm reactor, Water Sci. Technol. 40 (4–5) (1999) 161–168, https://doi.org/10.2166/wst.1999.0588.
[6] F. Iannacone, F. Di Capua, F. Granata, R. Gargano, G. Esposito, Shortcut nitrification-denitrification and biological phosphorus removal in acetate- and ethanol-fed moving bed biofilm reactors under microaerobic/aerobic conditions, Bioresour. Technol. 330 (2021) 124958, https://doi.org/10.1016/j.biortech.2021.124958.
[7] A. Tsitouras, N. Al-Ghussain, R. Delatolla, Two moving bed biofilm reactors in series for carbon, nitrogen, and phosphorous removal from high organic wastewaters, J. Water Process Eng. 41 (2021) 102088, https://doi.org/10.1016/j.jwpe.2021.102088.
[8] T. Saltnes, G. Sørensen, S. Eikås, Biological nutrient removal in a continuous biofilm process, Water Pract. Technol. 12 (4) (2017) 797–805, https://doi.org/10.2166/wpt.2017.083.
[9] M. Rodgers, X.M. Zhan, M.D. Burke, Nutrient removal in a sequencing batch biofilm reactor (SBBR) using a vertically moving biofilm system, Environ. Technol. 25 (2004) 211–218, https://doi.org/10.1080/09593330409355454.
[10] S. González-Martinez, P.A. Wilderer, Phosphate removal in a biofilm reactor, Water Sci. Technol. 23 (7–9) (1991) 1405–1415, https://doi.org/10.2166/wst.1991.0593.
[11] G. Pastorelli, R. Canziani, L. Pedrazzi, A. Rozzi, Phosphorus and nitrogen removal in moving-bed sequencing batch biofilm reactors, Water Sci. Technol. 40 (4–5) (1999) 169–176, https://doi.org/10.2166/wst.1999.0589.
[12] H.-S. Shin, H.-S. Park, Enhanced nutrient removal in porous biomass carrier sequencing batch reactor (PBCSBR), Water Sci. Technol. 23 (4–6) (1991) 719–728, https://doi.org/10.2166/wst.1991.0522.
[13] G. Petersen, H. Nour El-Din, E. Bundgaard, Second generation oxidation ditches: advanced technology in simple design, Water Sci. Technol. 27 (9) (1993) 105–113, https://doi.org/10.2166/wst.1993.0184.
[14] P. Ingildsen, C. Rosen, K.V. Gernaey, M.K. Nielsen, T. Guildal, B.N. Jacobsen, Modelling and control strategy testing of biological and chemical phosphorus removal at Avedøre WWTP, Water Sci. Technol. 53 (4–5) (2006) 105–113, https://doi.org/10.2166/wst.2006.115.
[15] C. Rosen, P. Ingildsen, T. Guildal, T.M. Nielsen, M.K. Nielsen, B.N. Jacobsen, H. A. Thomsen, Introducing biological phosphorus removal in an alternating plant by means of control: a full scale study, Water Sci. Technol. 53 (4–5) (2006) 133–141, https://doi.org/10.2166/wst.2006.117.
[16] R. Franci Gonçalves, F. Rogalla, Biological phosphorus removal in fixed films reactors, Water Sci. Technol. 25 (12) (1992) 165–174, https://doi.org/10.2166/wst.1992.0348.

[17] D. Pak, W. Chang, Simultaneous removal of nitrogen and phosphorus in a two-biofilter system, Water Sci. Technol. 41 (12) (2000) 101–106, https://doi.org/10.2166/wst.2000.0249.

[18] A. Shanableh, D. Abeysinghe, A. Hijazi, Effect of cycle duration on phosphorus and nitrogen transformations in biofilters, Water Res. 31 (1997) 149–153, https://doi.org/10.1016/S0043-1354(96)00230-8.

[19] P. Arnz, E. Arnold, P.A. Wilderer, Enhanced biological phosphorus removal in a semifull-scale SBBR, Water Sci. Technol. 43 (3) (2001) 167–174, https://doi.org/10.2166/wst.2001.0133.

[20] J. Ekholm, F. Persson, M. de Blois, O. Modin, M. Pronk, M.C.M. van Loosdrecht, C. Suarez, D.J.I. Gustavsson, B.-M. Wilén, Full-scale aerobic granular sludge for municipal wastewater treatment – granule formation, microbial succession, and process performance, Environ. Sci.: Water Res. Technol. 8 (2022) 3138–3154, https://doi.org/10.1039/D2EW00653G.

[21] J.C. Lopes, B.G. Silva, M.E.S. Dias, R.B. Carneiro, M.H.R.Z. Damianovic, E. Foresti, Enhanced biological nitrogen and phosphorus removal from sewage driven by fermented glycerol: comparative assessment between sequencing batch- and continuously fed-structured fixed bed reactor, Environ. Sci. Pollut. Res. 30 (2023) 11755–11768, https://doi.org/10.1007/s11356-022-23003-x.

[22] A. Franchi, D. Santoro, Current status of the rotating belt filtration (RBF) technology for municipal wastewater treatment, Water Pract. Technol. 10 (2) (2015) 319–327, https://doi.org/10.2166/wpt.2015.038.

[23] G. Bahreini, E. Elbeshbishy, J. Jimenez, D. Santoro, G. Nakhla, Integrated fermentation and anaerobic digestion of primary sludges for simultaneous resource and energy recovery: impact of volatile fatty acids recovery, Waste Manag. 118 (2020) 341–349, https://doi.org/10.1016/j.wasman.2020.08.051.

[24] E. Ossiansson, F. Persson, S. Bengtsson, M. Cimbritz, D.J.I. Gustavsson, Seasonal variations in acidogenic fermentation of filter primary sludge, Water Res. 242 (2023) 120181, https://doi.org/10.1016/j.watres.2023.120181.

[25] E. Ossiansson, S. Bengtsson, F. Persson, M. Cimbritz, D.J.I. Gustavsson, Primary filtration of municipal wastewater with sludge fermentation – impacts on biological nutrient removal, Sci. Total Environ. 902 (2023) 166483, https://doi.org/10.1016/j.scitotenv.2023.166483.

[26] A. di Biase, M.S. Kowalski, T.R. Devlin, J.A. Oleszkiewicz, Moving bed biofilm reactor technology in municipal wastewater treatment: a review, J. Environ. Manage. 247 (2019) 849–866, https://doi.org/10.1016/j.jenvman.2019.06.053.

[27] M. Henze, J. La Cour Jansen, Basic Biological Processes, in: J. La Cour Jansen, E. Arvin, M. Henze, P. Harremoës (Eds.), Wastewater Treatment - Biological and Chemical Processes, 4 ed., Polyteknisk Forlag, Copenhagen, 2019, pp. 59–129.

[28] A. Apprill, S. McNally, R. Parsons, L. Weber, Minor revision to V4 region SSU rRNA 806R gene primer greatly increases detection of SAR11 bacterioplankton, Aquat. Microb. Ecol. 75 (2015) 129–137, https://doi.org/10.3354/ame01753.

[29] A.E. Parada, D.M. Needham, J.A. Fuhrman, Every base matters: assessing small subunit rRNA primers for marine microbiomes with mock communities, time series and global field samples, Environ. Microbiol. 18 (2016) 1403–1414, https://doi.org/10.1111/1462-2920.13023.

[30] P.A. Castillo, S. González-Martínez, I. Tejero, Observations during start-up of biological phosphorus removal in biofilm reactors, Water Sci. Technol. 41 (4–5) (2000) 425–432, https://doi.org/10.2166/wst.2000.0475.

[31] D. Villard, I.A. Nesbø Goa, I. Leena Angell, S. Eikaas, T. Saltnes, W. Johansen, K. Rudi, Spatiotemporal succession of phosphorous accumulating biofilms during the first year of establishment, Water Sci. Technol. 88 (2) (2023) 381–391, https://doi.org/10.2166/wst.2023.214.

[32] C. Suarez, T. Rosenqvist, I. Dimitrova, C.J. Sedlacek, O. Modin, C.J. Paul, M. Hermansson, F. Persson, Biofilm colonization and succession in a full-scale partial nitritation-anammox moving bed biofilm reactor, Microbiome 12 (2024) 51, https://doi.org/10.1186/s40168-024-01762-8.

[33] S. Lücker, J. Schwarz, C. Gruber-Dorninger, E. Spieck, M. Wagner, H. Daims, Nitrotoga-like bacteria are previously unrecognized key nitrite oxidizers in full-scale wastewater treatment plants, ISME J. 9 (2015) 708–720, https://doi.org/10.1038/ismej.2014.158.

[34] S. Wegen, B. Nowka, E. Spieck, Low temperature and neutral pH define "*Candidatus Nitrotoga* sp." as a competitive nitrite oxidizer in coculture with *Nitrospira defluvii*, Appl. Environ. Microbiol. 85 (2019) e02569–18, https://doi.org/10.1128/AEM.02569-18.

[35] C.M. Singleton, F. Petriglieri, K. Wasmund, M. Nierychlo, Z. Kondrotaite, J. F. Petersen, M. Peces, M.S. Dueholm, M. Wagner, P.H. Nielsen, The novel genus, '*Candidatus* Phosphoribacter', previously identified as *Tetrasphaera*, is the dominant polyphosphate accumulating lineage in EBPR wastewater treatment plants worldwide, ISME J. 16 (2022) 1605–1616, https://doi.org/10.1038/s41396-022-01212-z.

[36] P.H. Nielsen, S.J. McIlroy, M. Albertsen, M. Nierychlo, Re-evaluating the microbiology of the enhanced biological phosphorus removal process, Curr. Opin. Biotechnol. 57 (2019) 111–118, https://doi.org/10.1016/j.copbio.2019.03.008.

[37] D. Villard, L. Snipen, K. Rudi, S. Branders, T. Saltnes, S. Eikås, W. Johansen, Transcriptional profiling elucidates biofilm functionality in the dynamic environment of an enhanced biological phosphorus removal reactor, Water Sci. Technol. 90 (7) (2024) 2114–2130, https://doi.org/10.2166/wst.2024.314.

[38] F.J. Rubio-Rincón, L. Welles, C.M. Lopez-Vazquez, M. Nierychlo, B. Abbas, M. Geleijnse, P.H. Nielsen, M.C.M. van Loosdrecht, D. Brdjanovic, Long-term effects of sulphide on the enhanced biological removal of phosphorus: the symbiotic role of *Thiothrix caldifontis*, Water Res. 116 (2017) 53–64, https://doi.org/10.1016/j.watres.2017.03.017.

[39] L. Ruiz-Haddad, M. Ali, M. Pronk, M.C.M. van Loosdrecht, P.E. Saikaly, Demystifying polyphosphate-accumulating organisms relevant to wastewater treatment: a review of their phylogeny, metabolism, and detection, Environ. Sci. Ecotechnol. 21 (2024) 100387, https://doi.org/10.1016/j.ese.2024.100387.

[40] C. Zhang, A. Guisasola, J.A. Baeza, A critical review on the effect of different carbon sources on EBPR: revaluation of performance and applications, Chem. Eng. J. 509 (2025) 161083, https://doi.org/10.1016/j.cej.2025.161083.

[41] C.M. Lopez-Vazquez, A. Oehmen, C.M. Hooijmans, D. Brdjanovic, H.J. Gijzen, Z. Yuan, M.C.M. van Loosdrecht, Modeling the PAO–GAO competition: effects of carbon source, pH and temperature, Water Res. 43 (2009) 450–462, https://doi.org/10.1016/j.watres.2008.10.032.

[42] H. Humbert, R. Lemaire, T. Germain, S. Lind, E. Gallimore, New generation of MBBR for biological treatment of carbon, nitrogen and phosphorus, Proc. Water Environ. Fed. 5 (2018) 551–558.

[43] A.B. Fanta, S. Sægrov, K. Azrague, S.W. Østerhus, Experimental investigation of simultaneous nitrification-denitrification and phosphorus removal in pilot-scale sequencing batch moving bed biofilm reactors (SB-MBBRs), Water Resour. Ind. 31 (2024) 100258, https://doi.org/10.1016/j.wri.2024.100258.

[44] C.M. López-Vázquez, C.M. Hooijmans, D. Brdjanovic, H.J. Gijzen, M.C.M. van Loosdrecht, A practical method for quantification of phosphorus- and glycogen-accumulating organism populations in activated sludge systems, Water Envir. Res. 79 (2007) 2487–2498, https://doi.org/10.2175/106143007X220798.

[45] A.J. Schuler, D. Jenkins, Enhanced biological phosphorus removal from wastewater by biomass with different phosphorus contents, part I: experimental results and comparison with metabolic models, Water Envir. Res. 75 (2003) 485–498, https://doi.org/10.2175/106143003X141286.

[46] V.A. Haaksman, E.J.H. van Dijk, S. Al-Zuhairy, M. Mulders, M.C.M. v. Loosdrecht, M. Pronk, Utilizing anaerobic substrate distribution for growth of aerobic granular sludge in continuous-flow reactors, Water Res. 257 (2024) 121531, https://doi.org/10.1016/j.watres.2024.121531.

[47] A.A. Cokro, Y. Law, R.B.H. Williams, Y. Cao, P.H. Nielsen, S. Wuertz, Non-denitrifying polyphosphate accumulating organisms obviate requirement for anaerobic condition, Water Res. 111 (2017) 393–403, https://doi.org/10.1016/j.watres.2017.01.006.

[48] A.B. Lanham, A. Oehmen, G. Carvalho, A.M. Saunders, P.H. Nielsen, M.A.M. Reis, Denitrification activity of polyphosphate accumulating organisms (PAOs) in full-scale wastewater treatment plants, Water Sci. Technol. 78 (12) (2018) 2449–2458, https://doi.org/10.2166/wst.2018.517.

[49] M. Gao, S. Sun, Q. Qiu, W. Zhou, L. Qiu, Enrichment denitrifying phosphorus-accumulating organisms in alternating anoxic-anaerobic/aerobic biofilter for advanced nitrogen and phosphorus removal from municipal wastewater, J. Water Process Eng. 55 (2023) 104089, https://doi.org/10.1016/j.jwpe.2023.104089.

[50] R. Marques, A. Ribera-Guardia, J. Santos, G. Carvalho, M.A.M. Reis, M. Pijuan, A. Oehmen, Denitrifying capabilities of *Tetrasphaera* and their contribution towards nitrous oxide production in enhanced biological phosphorus removal processes, Water Res. 137 (2018) 262–272, https://doi.org/10.1016/j.watres.2018.03.010.

[51] S. Kolakovic, E.B. Freitas, M.A.M. Reis, G. Carvalho, A. Oehmen, Accumulibacter diversity at the sub-clade level impacts enhanced biological phosphorus removal performance, Water Res. 199 (2021) 117210, https://doi.org/10.1016/j.watres.2021.117210.

[52] R. Diaz, B. Mackey, S. Chadalavada, J. kainthola, P. Heck, R. Goel, Enhanced bio-P removal: past, present, and future – a comprehensive review, Chemosphere 309 (2022) 136518, https://doi.org/10.1016/j.chemosphere.2022.136518.

[53] H. Joeng, E. Choi, Z. Yun, J.-B. Park, Practical aspects of nitrogen and phosphorous removal with floating media SBBR, J. Environ. Sci Heal. A. 38 (2003) 2135–2145, https://doi.org/10.1081/ESE-120023341.

[54] T. Hey, K. Jönsson, J. la Cour Jansen, Full-scale in-line hydrolysis and simulation for potential energy and resource savings in activated sludge – a case study, Environ. Technol. 33 (2012) 1819–1825, https://doi.org/10.1080/09593330.2011.650217.

[55] M. Henze, J. La Cour Jansen, Plants for biological phosphorus removal, in: J. La Cour Jansen, E. Arvin, M. Henze, P. Harremoës (Eds.), Wastewater Treatment - Biological and Chemical Processes, 4 ed., Polyteknisk Forlag, Copenhagen, 2019, pp. 259–271.

[56] M. Pronk, M.K. de Kreuk, B. de Bruin, P. Kamminga, R. Kleerebezem, M.C.M. van Loosdrecht, Full scale performance of the aerobic granular sludge process for sewage treatment, Water Res. 84 (2015) 207–217, https://doi.org/10.1016/j.watres.2015.07.011.

[57] F. Morgan-Sagastume, P. Eng, M. Piculell, H. Sánchez, P. Magnusson, D. Lamarre, S. Lind, Novel biofilm moving-bed system achieves simultaneous carbon removal and nitrification in municipal wastewater treatment, in: WEAO - Influents, Summer 2025, 2025, pp. 12–14.